How to Cite: Plotnikova, M.D., Shcherban′, M.G., Shitoeva, A.D., Vasyanin, A.N, & Shein, A.B. (2023) The Role of Surface Hydrophobization of Mild Steel by Some Triazole Derivatives in Acidic Medium. *Eurasian Journal of Chemistry, 4(112), 91-100.* https://doi.org/10.31489/2959-0663/4-23-9

Article

Received: 11 June 2023 | Revised: 16 October 2023 |
Accepted: 28 October 2023 | Published online: 15 November 2023

UDC 620.193.41; 621.3.011.212

https://doi.org/10.31489/2959-0663/4-23-9

Maria D. Plotnikova, Marina G. Shcherban′*, Anastasia D. Shitoeva, Alexander N. Vasyanin, Anatoly B. Shein

Perm State National Research University, Perm, Russia
*(*Corresponding author's e-mail: ma-sher74@mail.ru)*

The Role of Surface Hydrophobization of Mild Steel by Some Triazole Derivatives in Acidic Medium

Triazole derivatives (4,5-diphenyl-4H-1,2,4-triazole-3-thiol (4,5-PhTAT) and 3,4-diphenyl-5-(prop-2-yn-1-ylthio)-4H-1,2,4-triazole (3,4-PhPTTA) have been researched as corrosion inhibitors for mild steel in 0.1 N sulfuric acid solution. Electrochemical methods were used to estimate the corrosion rate and the inhibition efficiency: potentiodynamic polarization and impedance spectroscopy. The semi-empirical GFN2-xTB method, taking into account their implicit solvation in water using the ALPB method in the XTB program have been used for Geometry optimization of the structures of individual compounds and protomers in solution. Quantum chemical calculations suppose predominantly protonated structure for 3,4-PHPTTA molecules and neutral form of molecules for 4,5-PhTAT. According to electrochemical measurements the best inhibition efficiency for 4,5-PhTAT achieved at 50 $mg \cdot l^{-1}$and 200 $mg \cdot l^{-1}$ for 3,4-PhPTTA. 4,5-PhTAT and 3,4-PHPTTA are the mix-type inhibitors in 0.1 N sulfuric acid solution, but rate of cathodic process is decreased more than anodic. Contact angle measurements were carried out by the sessile drop method. Hydrophobization of the steel surface occurs in the blank acid and inhibited solution. The contact angle measurements by two test liquids (water and diethylene glycol) after corrosion with presents 4,5-Pstat and 3,4-PHPTTA show that the protective film formed in inhibited solution.

Keywords: corrosion, inhibitor, triazoles, polarization curves, surface tension, impedance spectroscopy, quantum chemical calculations, sessile drop method.

Introduction

Corrosion is a widely studied field of science. The use of inhibitors to control the corrosion in acid medium was found to have widespread applications [1–4]. The corrosion inhibition of steel in acidic medium by organic inhibitors was studied in considerable detail. Triazoles derivatives are N-heterocyclic compounds containing a five-member ring with three nitrogen atoms. Their molecules play important roles in biology due to their extensive biological interactions [4] and in chemistry due to their ability to inhibit corrosion of metals and alloys [1–3]. Today heterocycles inhibitors leading to minimize the corrosion process in metals [5–7]. The use of heterocycles inhibitors is of significant interest because of their economical synthesis methods and high protection efficiency [8, 9]. Among them, triazole derivatives have been researched as effective corrosion inhibitors for steel in acidic media [6, 7]. The inhibition efficiency depends on many factors: the nature of the metal surface, the inhibitor molecular structure — the number of adsorption active centers in the molecule, the charge density, the molecular size, and the ability of this molecule to interact with a metal surface. In order to understand action mechanisms of corrosion inhibitors, there are numerous experimental (electrochemical) [8, 9] and theoretical (quantum chemical) [10, 11] studies. One of the key approaches is the film theory of inhibitors [12, 13], according to the inhibition efficiency is due to the formation of a hydrophobic film on the metal surface. This film can be investigated by the sessile drop method [12–18]. The energy of the surface changes when the inhibitor film is formed and some adsorption centers appear and disappear on it. This can be measured by the method of steel surface contact angles with tested liquids and calculated the components (polar and dispersion) of the free surface energy with increase in the inhibitor concentration. The purpose of this work is to study the protective effect of some triazole derivatives against corrosion of low-carbon steel and to confirm the film theory of adsorption of organic heterocyclic corrosion inhibitors by both experimental electrochemical, surface physico-chemical methods and theoretical quantum chemical calculations.

Experimental

The tested inhibitors, namely 4,5-diphenyl-4H-1,2,4-triazole-3-thiol (4,5-PhTAT) and 3,4-diphenyl-5-(prop-2-yn-1-ylthio)-4H-1,2,4-triazole (3,4-PhPTTA), were synthesized according to a previously described experimental procedure [6, 18]. The concentration range of both inhibitors was 10–200 $mg \cdot l^{-1}$.

Geometry optimization of the structures of individual compounds was carried out using the semi-empirical GFN2-xTB method, taking into account their implicit solvation in water using the ALPB method in the XTB program [19, 20]. The calculation of the mole fractions of individual protomers in solution at 298.15 K was performed using the Boltzmann distribution based on the computed Gibbs energies of the optimized structures. The estimation of the protonation constants of compounds was done using the ChemAxon Marvin pK_a Plugin [21].

Electrochemical measurements were carried out using the electrochemical system Solatron 1280C. Steel potentials were measured relative to a silver chloride electrode. Potentiodynamic polarization and impedance measurements were performed using a glass electrochemical cell with an external space for silver chloride and counter platinum electrodes. Voltammetric studies were performed according to a three-electrode scheme in potentiodynamic mode at a working electrode potential sweep rate of 0.5 $mV \cdot s^{-1}$. Prior to polarization, the electrode was kept in the test solution for 30 min to establish a free corrosion potential, Ecor. Impedance measurements were recorded in the range of frequencies *f* from 20 kHz to 0.1 Hz, a sine wave with 5 mV amplitude was used to perturb the system. The criterion for estimating equivalent electrical circuits was the χ^2 parameter calculated in ZView2. A satisfactory equivalent scheme is for χ^2 less than 10^{-3} when weight coefficients calculated from experimental values of the impedance modulus. All potentials are reported vs standard hydrogen electrode.

Working electrodes with the composition, wt.%: Fe — 98.27; C — 0.20; Mn — 0.50; Si — 0.30; P — 0.04; S — 0.04; Cr — 0.15; Ni — 0.30; Cu — 0.20, were used in the study. The experiments were conducted in 0.1 N solution were prepared from chemically pure H_2SO_4 and distilled water.

The corrosion rate, *ICR* ($cm \cdot s^{-1}$), was estimated through the following equation combining Stern-Geary and Faraday equations:

$$ICR = (MB)/(zFS\rho R_p),$$

where *M* is average molecular weight of the metal or metal alloy ($g \cdot mol^{-1}$), *S* is the surface area (cm^2), *F* is the Faraday constant [96 485 $A \cdot s \cdot mol^{-1}$], *z* is the average charge of the metal, and ρ is the density of the metal ($g \cdot cm^3$), *B* is the Stern-Geary constant (V) defined as $B = b_a b_c/2.3(b_a + b_c)$, R_p is polarization resistance, (Ω). Units of corrosion rate in this paper are given in $mm \cdot year^{-1}$.

According to the theory of polarization resistance the R_p method is based on charge balance and the current-potential relationship (Tafel relationship) for electron-transfer reactions. R_p is defined as the differential of the overpotential, Δ*E* (volt), over the withdrawn current, i_{corr} (amp), when the slope of polarization curves at the corrosion potential:

$$R_p = dE/di = b_a b_c /2.3 i_{cor}(b_a + b_c) = B/i_{corr},$$

where b_a and b_c are anodic and cathodic Tafel constants (volt), i_{corr} is the corrosion current ($A \cdot cm^{-2}$) [22, 23].

The inhibition efficiency for each concentration of inhibitors was calculated according to the equation,

$$IE(\%) = (1 - i_{corr}/i_{0corr}) \cdot 100,$$

where *IE,* is the inhibition efficiency, i_{corr} and i_{0corr} are the corrosion current densities ($A \cdot cm^{-2}$) with and without inhibitor, respectively. The corrosion current density (i_{corr}) was determined by extrapolating the Tafel lines.

On the basis of Young's equation plus Owen-Wendt's theory, the surface free energies of the steel surface can be calculated using the contact angles between the two test liquids (water and diethylene glycol) and steel surface [24, 25]. Contact angle measurements were carried out using a tensiometer DSA 25E (KRUSS) by the sessile drop method [26]. Test liquids (liquid with known the value of surface tension) were dropped to the surface of the sample using a dispenser, after that the angle between three phases (steel, test liquid and air) was measured. The volume of test liquids was 1–2 μl. All the experiments were carried out after immersion of mild steel for 24 hours in 0.1 N H_2SO_4 in absence and presence of different concentrations of inhibitors. After immersion samples were cleaned with distilled water repeatedly and dried in hot air, then the contact angles were measured.

Results and Discussion

Based on the structural characteristics of 4,5-PhTAT, it is reasonable to posit that this compound exhibits amphiprotic behavior in aqueous systems, where it can undergo both protonation and deprotonation reactions. According to free energy calculations, the tautomeric form with proton moved to the N atom dominates in the neutral state (Fig. 1).

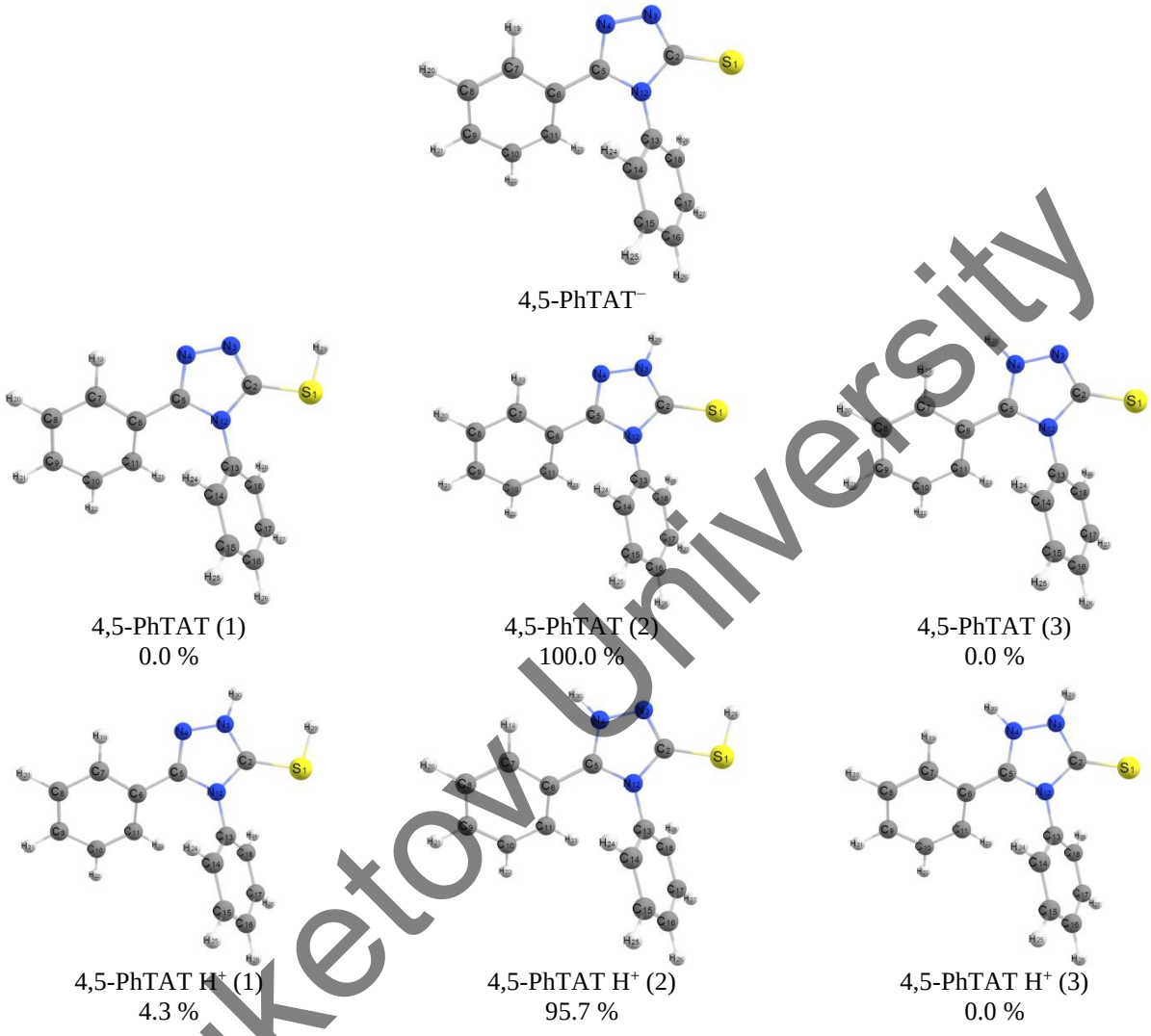

Figure 1. The optimized geometries of the deprotonated molecule (anion) 4,5-PhTAT, as well as the tautomers of the neutral molecule and its mono-protonated form obtained at the GFN2-xTB[ALPB(H_2O)] theory level with their relative fractions (%) in solution at 298.15 K

The protonation/deprotonation equilibrium constants were computed using the Marvin pK_a Plugin program, taking into account tautomerization. The results indicate that deprotonation is the only feasible outcome in solutions with weakly alkaline properties (pK_a = 7.21). Conversely, the calculations strongly suggest that protonation is practically unattainable, as evidenced by the extremely low predicted value of the corresponding equilibrium constant (pK_a = –4.65). Notably, the calculations reveal that among the three feasible tautomers of the protonated form present in solution, the 4,5-PhTAT H^+ (2) tautomer is expected to be the predominant species.

Protonation of 3,4-PHPTTA

Only protonation processes are possible for 3,4-PHPTTA. In contrast to 4,5-PhTAT, protonation of 3,4-PHPTTA is entirely possible in strongly acidic aqueous solutions (with a pKa value of 0.97 for the 3,4-PHPTTA H^+(1) form and 0.22 for the 3,4-PHPTTA H^+(2) form). The calculation of the molar fraction of monoprotonated forms using the GFN2-xTB[ALPB(H_2O)] method agrees well with the results obtained from the Marvin pK_a Plugin and confirms the predominance of the 3,4-PHPTTA H^+ (1) protomer (Fig. 2).

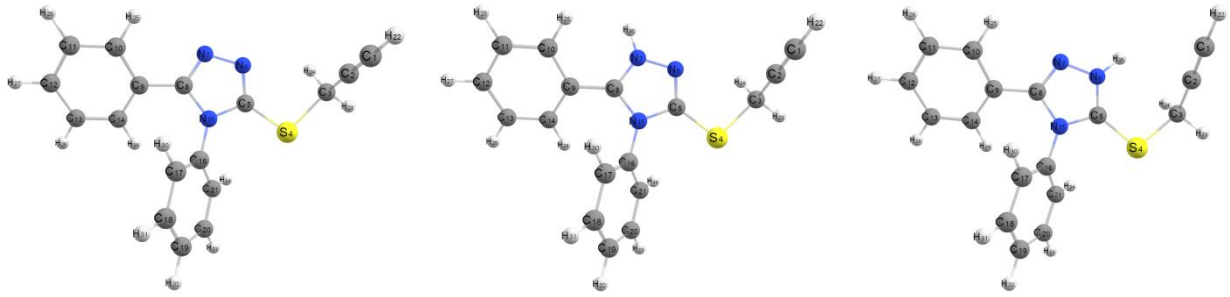

3,4-PHPTTA | 3,4-PHPTTA H^+(1) 89.3 % | 3,4-PHPTTA H^+(2) 10.7 %

Figure 2. The optimized geometries of the neutral molecule 3,4-PHPTTA and its monoprotonated tautomers obtained at the GFN2-xTB[ALPB(H_2O)] level of theory with their relative fractions (%) in solution at 298.15 K

Based on the results of the calculations, it was shown that in acidic H_2SO_4 solutions, inhibitors 4,5-PhTAT and 3,4-PHPTTA exist in different forms: 3,4-PHPTTA molecules are predominantly protonated, while 4,5-PhTAT exists as neutral molecules.

Polarization curves for mild steel in 0.1 N H_2SO_4 solution without and with addition of 100 mg·l^{-1} of 4,5-PhTAT and 3,4-PhPTTA are shown in Figure 3.

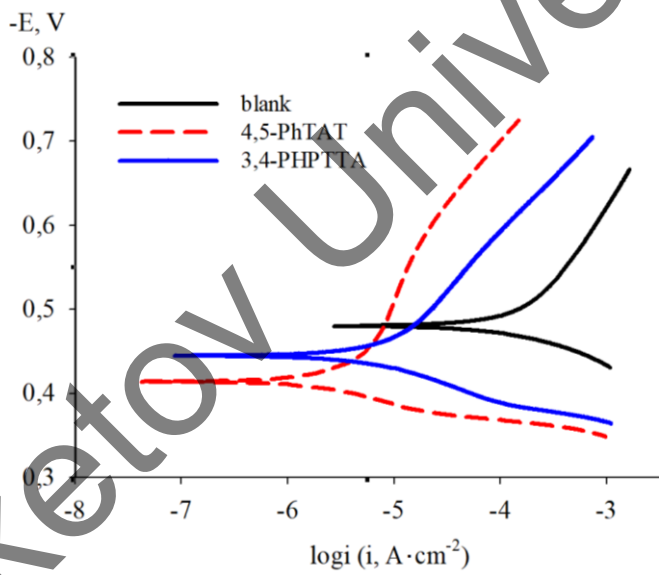

Figure 3. Potentiodynamic polarization curves for mild steel in 0.1 N H_2SO_4 with different triazole derivatives

Analysis of Figure 3 and Table 1 reveals that the presence of both triazoles resulted in a shift of the corrosion potential towards the anodic direction in comparison with the result obtained in the blank acid solution (Table 1). The anodic and the cathodic current densities were decreased, indicating that 4,5-PhTAT and 3,4-PhPTTA suppressed both the anodic and cathodic reactions (Fig. 3).

Table 1 shows that in the case of 4,5-PhTAT corrosion current decreased already at 10 mg·l^{-1} and had minimal value at 50 mg·l^{-1}, then it slightly increased with the growth concentration. If added to the system 3,4-PhPTTA, corrosion currents slowly decrease with increasing concentration, it appears from 50 mg·l^{-1}.

Figure 3 demonstrates that polarization curves show two linear parts in the anode region in the presence of inhibitors, but Table 1 shows only Tafel coefficients near by corrosion potential. It is shown that, the injection of inhibitors decreased the rate of cathode process greater than anodic, as the b_c has increased with raising concentration. According to linear polarization results, the corrosion rate decreases from 1.13 mm·year^{-1} to 0.023 and 0.049 mm·year^{-1} (47 and 23 times) with presence 4,5-PhTAT and 3,4-PhPTTA respectively.

Table 1

Polarization Parameters for Mild Steel in 0.1 N H_2SO_4 Solution Containing Different Concentrations of 4,5-PhTAT and 3,4-PhPTTA at 298 K

Inhibitor	C, mg·l^{-1}	Tafel polarization				Linear polarization	
		$-E_{corr}$, mV	i_{corr}, A·cm^{-2}	b_a, mV	b_c, mV	R_p, Ω	ICR, mm·year^{-1}
–	–	677	$8.34 \cdot 10^{-5}$	51	125	190	1.13
4,5-PhTAT	10	625	$3.56 \cdot 10^{-5}$	53	132	2994	0.041
	50	619	$2.45 \cdot 10^{-6}$	55	140	5154	0.023
	100	614	$2.09 \cdot 10^{-6}$	54	160	4831	0.024
	200	604	$2.87 \cdot 10^{-6}$	51	189	4466	0.033
3,4-PhPTTA	10	672	$8.10 \cdot 10^{-5}$	48	120	200	1.25
	50	654	$9.19 \cdot 10^{-6}$	45	130	1603	0.11
	100	645	$7.15 \cdot 10^{-6}$	47	158	1943	0.083
	200	601	$4.18 \cdot 10^{-6}$	50	157	2493	0.049

Figure 4 shows the Nyquist diagrams of impedance data of mild steel in 0.1 N sulfuric acid solution with different concentrations 4,5-PhTAT and 3,4-PhPTTA. Impedance spectra in pure acid solution are presented as the insertion on one of the diagrams. These diagrams (Fig. 4) at E_{corr} are characterized by a depressed capacitive semicircle at high to medium frequencies. The dispersion is explained by surface heterogeneity due to surface roughness [26, 27]. Hence the inhibition efficiency has a tendency to grow as the values of R_{ct} increase.

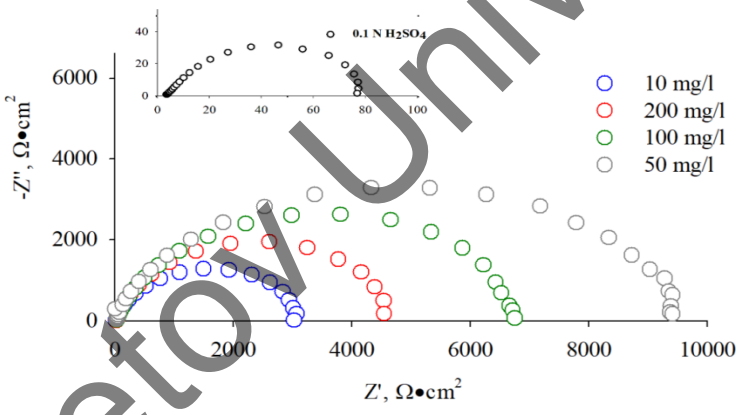

(*a*)

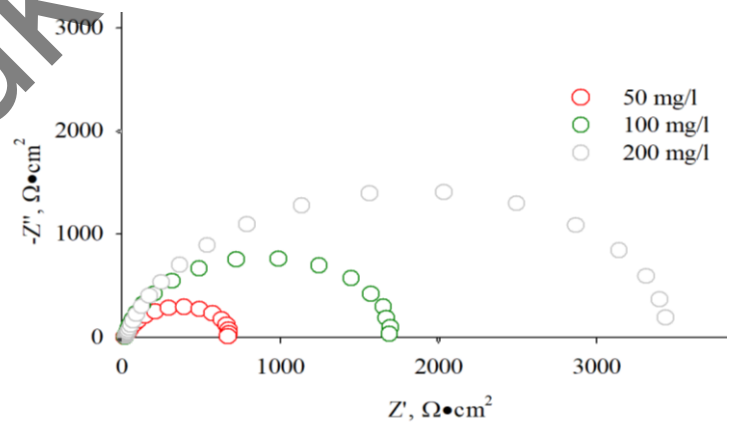

(*b*)

Figure 4. Nyquist diagrams of mild steel in a solution of 0.1 N H_2SO_4 at E_{corr} with addition of various concentration of (*a*) and (*b*) 3,4-PhPTTA

The calculation results correlate with the electrochemical results. 4,5-PhTAT gives a greater inhibition efficiency than 3,4-PhPTTA at low concentration due to the neutral form of molecules. The protonated form of 3,4-PhPTTA molecules at low concentration are pushed off the surface of mild steel with positive charge in sulfuric acid solution.

The calculation of the free surface energy (SFE) of steel was carried out before and after contact with a corrosive medium to confirm the assumptions about the formation of the protective film and the chemical nature of adsorption. The value of SFE due to the isolation of its polar (γ^p) and dispersion (γ^d) components can indicate the direction of further modification to increase resistance of the corrosion system.

The surface energy parameters were calculated based on the analysis of the Owen-Wendt's equation:

$$W_a = \gamma_{LG}(1 + \cos\theta_C) = 2(\gamma^d_{SG}\,\gamma^d_{LG})^{0,5} + 2(\gamma^p_{SG}\,\gamma^p_{LG})^{0,5},$$

where W_a — work of adhesion, γ_{LG} — the liquid/air interfacial tension, γ^d_{SG}, γ^p_{SG} — polar and dispersive component of surface energies of steel, γ^p_{LG}, γ^d_{LG} — polar and dispersive component of surface tension of test liquids, $\cos\theta_C$ — the contact angle for test liquids at steel surface after corrosion.

Figure 5 demonstrates images of test liquids drops on the steel surface after exposition in corrosion medium with inhibitors during 24 hours.

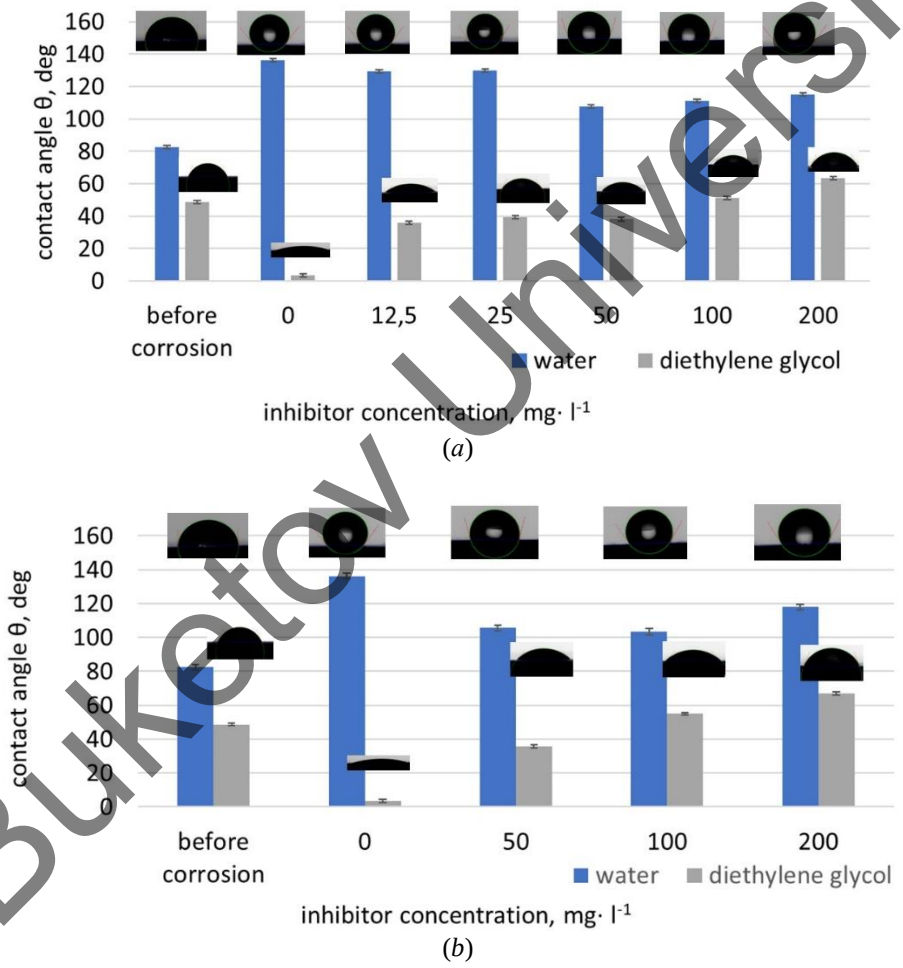

Figure 5. Surface wettability of steel surface after corrosion in 0.1 N H_2SO_4 solution with (*a*) 4,5-PhTAT and (*b*) 3,4-PhPTTA

In general, the steel surface before corrosion has a hydrophilic character, since metals and metal alloys have high surface energy values and wettability by liquids with lower surface tensions. Thus, the surface energies of ferrite and cementite are 2482 and 2050 mJ·m^{-2} [25], these steel phases are wetted by water with surface tension 72 mJ·m^{-2} [28]. According to [29], the contact angle of mild steels by water is about 64° [30]. In our case, the contact angle is 82°, this value is close to the contact angle on pyrolytic graphite (83.9°). This allows to propose that the surface is enriched by carbon.

The contact angle increased to 136° after exposure of samples in pure sulfuric acid that leads to surface hydrophobization significantly. After that surface roughness increased as a result of iron dissolution and surface enrichment by carbon — the contact angles are close to those of fine-dispersed graphite and graphene [28, 29]. The hydrophobicity is also shown by the wettability of the steel by less polar liquid after immersion in pure acid. The contact angles decrease from 48° to 3°, if the test liquid is changed from water to diethylene glycol.

The steel surface is also hydrophobized in the presence of the inhibitors (contact angles range from 105° to 130°); however, this is caused by other reasons. In this case, the hydrophobicity increased probably due to the formation of a protective film of inhibitor on the steel surface. The contact angle of the primary steel surface is 48,7°±0,9°, then after corrosion in sulfuric acid it is decreased to 3,6°±0,5° and finally the contact angle in presence of inhibitors changes in the range of 35–70°. There is a tendency to growth with increasing inhibitor concentration.

These changes in the wettability of test liquids after corrosion indicate a different state of steel surface. Figure 6 demonstrates the redistribution of the polar and dispersion components of the free surface energy, its values and the inhibition efficiency are given in Table 2.

The immersion of the samples in blank sulfuric acid leads to significant hydrophobization of the steel surface, the contact angle increases to 136° as a result of the dissolution of iron and the surface enrichment with carbon [31-33].

The steel surface in the presence of an inhibitor is also hydrophobized — the contact angles are in the range of 105° — 130°. Probably, the effect of hydrophobization of the surface is associated with the formation of a protective film of the inhibitor, and not with the increase of the carbon concentration on the steel surface.

Also the ratio of the polar and dispersion components of the free surface energy changes when samples are kept in inhibited acid. Calculated SFE values and the degrees of protection calculated from the results of weight loss testing are presented in Table 2.

Table 2

Surface energies for test liquids (22° C) and degree of protection of St3 after weight loss tests in the presence of triazole derivatives in 0.1 N H_2SO_4 solution

Conc., mg·l^{-1}	γ^p_{SG}, mJ·m^{-2}	γ^d_{SG}, mJ·m^{-2}	γ_{SG}, mJ·m^{-2}	$\gamma^d_{SG}/\gamma^p_{SG}$	Z, %
Before immersion	6,2	24,98	31,18	4,0	
0	43,4	149,96	193,32	3,5	
4,5-PhTAT					
50	3,73	70,19	73,92	18,8	96
100	6,40	78,18	84,58	12,2	92
200	9,25	83,96	93,21	9,1	92
3,4-PhPTTA					
50	1,13	53,40	54,53	47,3	94
100	1,06	42,12	43,18	39,7	95
200	2,53	43,28	45,82	17,3	95

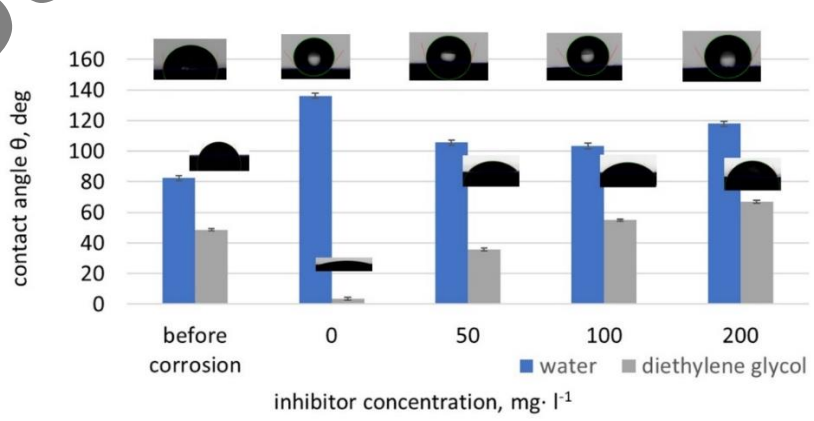

Figure 6. The effect of redistribution of the free surface energy with increasing concentration of inhibitors

4,5-PhTAT has higher value of ratio dispersion and polar components of the free surface energy (Table 2). 4,5-PhTAT forms hydrophobic film at low concentration and, due to this, has inhibition properties already at 10 mg·l^{-1}. 3,4-PhPTTA doesn't have inhibition activity at low concentration.

Conclusions

1. 4,5-diphenyl-4H-1,2,4-triazole-3-thiol (4,5-PhTAT) and 3,4-diphenyl-5-(prop-2-yn-1-ylthio)-4H-1,2,4-triazole (3,4-PhPTTA) act as good inhibitors for mild steel in 0.1 N H_2SO_4, the rate of corrosion is reduced by 47 and 23 times, respectively. The inhibition efficiency depended from concentration: 4,5-PhTAT has the best inhibition efficiency value at 50 mg·l^{-1} and 3,4-PhPTTA only at 200 mg·l^{-1}.

2. Polarization curves proved that 4,5-PhTAT and 3,4-PhPTTA were mixed type inhibitors, but which can suppress cathodic reactions more. Impedance plots indicated that Rct values increase as well as shown in polarization results. Theoretical calculations provide good support to experimental electrochemical results.

3. The steel surface in the presence of both compounds becomes more hydrophobic, as the contact angle increases from 82° to 120° — 130° depending on the inhibitor concentration. Also, the free surface energy of steel decreases in the presence of inhibitors compared to pure acid (from 193 mJ·m^{-2} to 46 — 74 mJ·m^{-2}), and the SFE components are redistributed: the contribution of the dispersion component with adding triazole derivatives in corrosion media to the total value of SFE increases by 3-4 times compared to the test steel surface.

4. Redistribution in polar and dispersion components consist of different forms of molecular existence: 3,4-PHPTTA is predominantly protonated, while 4,5-PhTAT is neutral molecules according to quantum chemical calculation.

Acknowledgments

The research was supported by the PERM SCIENTIFIC AND EDUCATION CENTRE "RATIONAL SUBSOIL USE", 2023.

References

1 Awad, M.K., Mustafa, M.R., & Elnga, M.M.A. (2010). Computational simulation of the molecular structure of some triazoles as inhibitors for the corrosion of metal surface. *Journal of molecular structure: theochem*, *959*(1-3), 66-74. https://doi.org/10.1016/j.theochem.2010.08.008

2 Ouicia, H., Tourabib, M., Benalic, O., Sellesd, C., Jamae, C., Zarroukf, A., & Bentiss, F. (2017). Adsorption and corrosion inhibition properties of 5-amino 1,3,4-thiadiazole-2-thiol on the mild steel in hydrochloric acid medium: Thermodynamic, surface and electrochemical studies. *Journal of Electroanalytical Chemistry*, *803*, 125-134. http://dx.doi.org/10.1016/j.jelechem.2017.09.

3 Hrimla, M., Bahsis, L., Laamari, M. R., Julve, M., & Stiriba, S. E. (2021). An overview on the performance of 1, 2, 3-triazole derivatives as corrosion inhibitors for metal surfaces. *International Journal of Molecular Sciences*, *23*(1), 16. https://doi.org/10.3390/ijms23010016

4 Bozorov, K., Zhao, J., & Aisa, H.A. (2019) 1,2,3-Triazole-containing hybrids as leads in medicinal chemistry: A recent overview. *Bioorg. Med. Chem.*, *27 (16)*, 3511–3531. https://doi.org/10.1016/j.bmc.2019.07.005

5 Plotnikova, M.D., Solovyev, A.D., Shein, A.B., Bakiev, A.N., & Sofronov, A.S. (2021). New inhibitors based on substituted 1, 2, 4-triazoles for mild steel in hydrochloric acid solutions. *International Journal of Corrosion and Scale Inhibition*, *10*(3), 1230-1244. https://doi.org/10.17675/2305-6894-2021-10-3-23

6 Plotnikova, M.D., Shitoeva, A.D., Solovyev, A.D., Shein, A.B., & Bakiev, A.N. (2023). Some aspects of the of the mechanism of C1018 steel protection in hydrochloric acid solutions by triazole derivatives. *Int. J. Corros. Scale Inhib.*, *2023*, *12*, no. 2, 511–530. https://doi.org/10.17675/2305-6894-2023-12-2-8

7 Hrimla, M., Bahsis, L., Boutouil, A., Laamari, M.R., Julve, M., & Stiriba, S.E. (2021). Corrosion inhibition performance of a structurally well-defined 1, 2, 3-triazole derivative on mild steel-hydrochloric acid interface. *Journal of Molecular Structure*, *1231*, 129895. doi.org/10.1016/j.molstruc.2021.129895

8 Carranza, M.S.S., Reyes, Y.I.A., Gonzales, E.C., Arcon, D.P., & Franco, F.C. (2021). Electrochemical and quantum mechanical investigation of various small molecule organic compounds as corrosion inhibitors in mild steel. *Heliyon*, *7*(9). doi: 10.1016/j.heliyon.2021.e07952

9 Fouda, A.S., Wahba, A.M., & Al-Bonayan, A.M. (2021). Corrosion inhibition of stainless steel in 1.0 M hydrochloric acid solution using novel nonionic surfactant: electrochemical and density functional Theory/B3LYP/6-31G* analysis. *Surface Engineering and Applied Electrochemistry*, *57*, 689-702. https://doi.org/10.3103/S1068375521060041

10 Hamani, H., Daoud, D., Benabid, S., & Douadi, T. (2022). Electrochemical, density functional theory (DFT) and molecular dynamic (MD) simulations studies of synthesized three news Schiff bases as corrosion inhibitors on mild steel in the acidic environment. *Journal of the Indian Chemical Society*, *99*(7), 100492. https://doi.org/10.1016/j.jics.2022.100492

11 Akpan, E.D., Oladipo, S.D., Quadri, T.W., Olasunkanmi, L.O., Nwanna, E.E., Omondi, B., & Ebenso, E.E. (2022). Formamidine-Based Thiuram Disulfides as Efficient Inhibitors of Acid Corrosion of Mild Steel: Electrochemical, Surface, and Density Functional Theory/Monte Carlo Simulation Studies. *ACS omega*, *7*(30), 26076-26091. https://doi.org/10.1021/acsomega.2c00985

12 Liu, P., Huang, X., & Guo Zh. (2023). Superhydrophobic Corrosion Inhibitor Intercalated Hydrotalcite Coating for Enhanced Corrosion Resistance of the Aluminum. *ACS Applied Engineering Materials*, *1*(1), 486-494. https://doi.org/10.1021/acsaenm.2c00117

13 Kai An, Wei Tong, Youqiang Wang, Yongquan Qing, Yi Sui, Ying Xu, & Chenbing Ni. (2023). Eco-Friendly Superhydrophobic Coupling Conversion Coating with Corrosion Resistance on Magnesium Alloy. *Langmuir*, *39*(18), 6355-6365. https://doi.org/10.1021/acs.langmuir.3c00025

14 Barkhudarov, P.M., Shah, P.B., Watkins, E.B., Doshi, D.A., Brinker, C.J., & Majewski, J. (2008). Corrosion inhibition using superhydrophobic films. *Corrosion Science*, *50*(3), 897-902. https://doi.org/10.1016/j.corsci.2007.10.005

15 Pandarinathan, V., Lepkova, K., Bailey, S., Becker, T., & Gubner, R. (2014). Adsorption of corrosion inhibitor 1-dodecylpyridinium chloride on carbon steel studied by in situ AFM and electrochemical methods. *Industrial and Engineering Chemistry Research*, *53*(14), 5858-5865. https://doi.org/10.1021/ie402784y

16 Umoren, S.A., Obot, I.B., Madhankumar, A., & Gasem, Z.M. (2015). Performance evaluation of pectin as ecofriendly corrosion inhibitor for X60 pipeline steel in acid medium: Experimental and theoretical approaches. *Carbohydrate Polymers*, *100*(124), 280-291. https://doi.org/10.1016/j.carbpol.2015.02.036

17 Ma, X., Dang, R., Kang, Y. H., Gong, Y., Luo, J., Zhang, Y. Y.,... & Ma, Y. J. (2020). Electrochemical studies of expired drug (formoterol) as oilfield corrosion inhibitor for mild steel in H2SO4 media. *International Journal of Electrochemical Science*, *15*, 1964-1981. https://doi.org/10.20964/2020.03.65

18 Plotnikova, M.D., Solovyev, A.D., Shein, A.B., Vasyanin, A.N. & Sofronov, A.S. (2021). Corrosion inhibition of mild steel by triazole and thiadiazole derivatives in 5 M hydrochloric acid medium. *Int. J. Corros. Scale Inhib.*, *9*(3), 1336–1354. https://doi.org/10.17675/2305-6894-2021-10-3-29

19 C. Bannwarth, E. Caldeweyher, S. Ehlert, A. Hansen, P. Pracht, J. Seibert, S. Spicher, & S. Grimme. (2021). Extended tight-binding quantum chemistry methods. *WIREs Computational Molecular Science*, 11, 1493. https://doi.org/10.1002/wcms.1493

20 C. Bannwarth, S. Ehlert, & S. Grimme. (2019). GFN2-xTB—An Accurate and Broadly Parametrized Self-Consistent Tight-Binding Quantum Chemical Method with Multipole Electrostatics and Density-Dependent Dispersion Contributions, *J. Chem. Theory Comput*, 15, 1652–1671. https://doi.org/10.1021/acs.jctc.8b01176.

21 Caine, B.A., Dardonville, Ch., & Popelier, L.A. (2018). Prediction of Aqueous pKa Values for Guanidine-Containing Compounds Using Ab Initio Gas-Phase Equilibrium Bond. *ACS Omega*, 3, 3835−3850. https://doi.org/10.1021/acsomega.8b00142

22 Ma, I.W., Ammar, S., Kumar, S.S., Ramesh, K., & Ramesh, S. (2022). A concise review on corrosion inhibitors: types, mechanisms and electrochemical evaluation studies. *Journal of Coatings Technology and Research*, 1-28. https://doi.org/10.1007/s11998-021-00547-0

23 Hsieh, M.-K., Dzombak, D.A., & Vidic, R.D. (2010). Bridging Gravimetric and Electrochemical Approaches To Determine the Corrosion Rate of Metals and Metal Alloys in Cooling Systems: Bench Scale Evaluation Method. Industrial & amp. *Engineering Chemistry Research*, *49*(19), 9117–9123. https://doi.org/10.1021/ie100217k

24 Owens, D.K. & Wendt, R.C. (1969). Estimation of the Surface Free Energy of Polymers. *J. Appl. Polym. Sci.*, *13*(8), 1741–1747. https://doi.org/10.1016/0006-2952(75)90009-x

25 Ponomar, M., Krasnyuk, E., Butylskii, D., Nikonenko, V., Wang, Y., Jiang, C.,... & Pismenskaya, N. (2022). Sessile drop method: critical analysis and optimization for measuring the contact angle of an ion-exchange membrane surface. *Membranes*, *12*(8), 765. https://doi.org/10.3390/membranes12080765

26 Growcock, F.B., & Jasinski, R.J. (1989). Time-resolved impedance spectroscopy of mild steel in concentrated hydrochloric acid. *Journal of the Electrochemical Society*, *136*(8), 2310. https://doi.org/10.1149/1.2097847

27 Popova, A., & Christov, M. (2006). Evaluation of impedance measurements on mild steel corrosion in acid media in the presence of heterocyclic compounds. *Corrosion Science*, *48*(10), 3208-3221. https://doi.org/10.1016/j.corsci.2005.11.001

28 Song, E.J., Bhadeshia, H.K.D.H., & Suh, D.W. (2013). Effect of hydrogen on the surface energy of ferrite and austenite. *Corrosion Science*, *77*, 379-384. https://doi.org/10.1016/j.corsci.2013.07.043

29 Kalová, J., & Mareš, R. (2015). Reference values of surface tension of water. *International Journal of Thermophysics*, *36*, 1396-1404. https://doi.org/10.1007/s10765-015-1907-2

30 Duan, C., Zhu, Y., Gu, W., Li, M., Zhao, D., Zhao, Z.,... & Wang, Y. (2018). Atomic coupling growth of graphene on carbon steel for exceptional anti-icing performance. *ACS Sustainable Chemistry & Engineering*, *6*(12), 17359-17367. https://doi.org/10.1021/acssuschemeng.8b04913

31 Bañon, F., Montaño, R., Vazquez-Martinez, J. M., & Salguero, J. (2022). Free surface energy evaluation in the laser texturing of a carbon steel s275. *Procedia CIRP*, *108*, 72-76. https://doi.org/10.1016/j.procir.2022.03.016

32 Shin, Y.J., Wang, Y., Huang, H., Kalon, G., Wee, A.T.S., Shen, Z.,... & Yang, H. (2010). Surface-energy engineering of graphene. *Langmuir*, *26*(6), 3798-3802. https://doi.org/10.1021/la100231u

33 Kozbial, A., Li, Z., Conaway, C., McGinley, R., Dhingra, S., Vahdat, V., … & Li, L. (2014). Study on the surface energy of graphene by contact angle measurements. *Langmuir*, *30*(28), 8598-8606. https://doi.org/10.1021/la5018328

Information about authors*

Plotnikova, Maria Dmitrievna — Candidate of chemical sciences, Assistant Professor of Physical Chemistry Department, Perm State National Research University, Bukireva st., 15, 614990, Perm, Russia; e-mail: plotnikova-md@mail.ru; https://orcid.org/0000-0002-4050-5682

Shcherban', Marina Grigoryevna (*corresponding author*) — Candidate of chemical sciences, Assistant professor of Physical Chemistry Department, Perm State National Research University, Bukireva st., 15, 614990, Perm, Russia; e-mail: ma-sher74@mail.ru; https://orcid.org/0000-0002-6905-6622

Shitoeva, Anastasia Dmitrievna — First-Year Master Student, Perm State National Research University, Bukireva st., 15, 614990, Perm, Russia; e-mail: shitoeva0910@gmail.com; https://orcid.org/0009-0005-9611-7848

Vasyanin, Alexander Nikolaevich — Candidate of chemical sciences, Assistant professor of Physical Chemistry Department, Perm State National Research University, Bukireva st., 15, 614990, Perm, Russia; e-mail: avasyanin@psu.ru; https://orcid.org/0000-0002-1991-094X

Shein, Anatoly Borisovich — Doctor of chemical sciences, Professor of Physical Chemistry Department, Perm State National Research University, Bukireva st., 15, 614990, Perm, Russia; e-mail: ashein@psu.ru; https://orcid.org/0000-0002-2102-0436

*The author's name is presented in the order: *Last Name, First and Middle Names*